Heliyon

Received:
10 October 2017
Revised:
28 December 2017
Accepted:
16 February 2018

Cite as:
Ma. Cristina Acosta-García, Israel Morales-Reyes, Anabel Jiménez-Anguiano, Nikola Batina, N. P. Castellanos, R. Godínez-Fernández. Simultaneous recording of electrical activity and the underlying ionic currents in NG108-15 cells cultured on gold substrate. Heliyon 4 (2018) e00550. doi: 10.1016/j.heliyon.2018.e00550

Simultaneous recording of electrical activity and the underlying ionic currents in NG108-15 cells cultured on gold substrate

Ma. Cristina Acosta-García [a,b], Israel Morales-Reyes [c,d], Anabel Jiménez-Anguiano [b], Nikola Batina [c], N. P. Castellanos [d], R. Godínez-Fernández [d,*]

[a] *Posgrado en Biología Experimental, División de Ciencias Biológicas y de la Salud, Universidad Autónoma Metropolitana-Iztapalapa, México City, Mexico*

[b] *Departamento de Biología de la Reproducción, Universidad Autónoma Metropolitana-Iztapalapa, México City, Mexico*

[c] *Laboratorio de Nanotecnología e Ingeniería Molecular, Departamento de Química, Universidad Autónoma Metropolitana-Iztapalapa, México City, Mexico*

[d] *Laboratorio de Biofísica, Departamento de Ingeniería eléctrica, Universidad Autónoma Metropolitana-Iztapalapa, México City, Mexico*

[*] Corresponding author.
E-mail address: gfjr@xanum.uam.mx (R. Godínez-Fernández).

Abstract

This paper shows the simultaneous recording of electrical activity and the underlying ionic currents by using a gold substrate to culture NG108-15 cells. Cells grown on two different substrates (plastic Petri dishes and gold substrates) were characterized quantitatively through scanning electron microscopy (SEM) as well as qualitatively by optical and atomic force microscopy (AFM). No significant differences were observed between the surface area of cells cultured on gold substrates and Petri dishes, as indicated by measurements performed on SEM images. We also evaluated the electrophysiological compatibility of the cells through standard patch-clamp experiments by analyzing features such as the resting potential, membrane resistance, ionic currents, etc. Cells grown on both

https://doi.org/10.1016/j.heliyon.2018.e00550

substrates showed no significant differences in their dependency on voltage, as well as in the magnitude of the Na+ and K+ current density; however, cells cultured on the gold substrate showed a lower membrane capacitance when compared to those grown on Petri dishes. By using two separate patch-clamp amplifiers, we were able to record the membrane current with the conventional patch-clamp technique and through the gold substrate simultaneously. Furthermore, the proposed technique allowed us to obtain simultaneous recordings of the electrical activity (such as action potentials firing) and the underlying membrane ionic currents. The excellent conductivity of gold makes it possible to overcome important difficulties found in conventional electrophysiological experiments such as those presented by the resistance of the electrolytic bath solution. We conclude that the technique here presented constitutes a solution to the problem of the simultaneous recording of electrical activity and the underlying ionic currents, which for decades, had been solved only partially.

Keywords: Biophysics, Cell biology

1. Introduction

The use of biomaterials has become increasingly important for the design of new medical devices, where it is extremely important to have a deep understanding of both its constitution and properties. In this regard, biocompatibility is a key aspect that should be always addressed. One of the materials recently proposed as a substrate for cell culturing is gold. In fact, several excitable cells have been successfully cultured on gold electrodes (Nam et al., 2004; Heller et al., 2005; Brunetti et al., 2010; Mrksich et al., 1996; Romanova et al., 2006; Soussou et al., 2007; Coletti et al., 2009; Yoon and Mofrad, 2011). However, to our knowledge, a systematical study of the effects of gold on the electrical properties of cells as well as a detailed study of its electrophysiological biocompatibility are still missing. In spite of this, there are some good reasons for using gold as a substrate: it is a noble metal that does not readily react with salts and molecules found in physiological solutions; it does not react with cellular material and it is a biocompatible material. Moreover, as has been shown in recent studies, it possesses interesting features that make it suitable for atomic force microscopy (AFM) studies of the morphological properties of cells at a molecular level (flat gold substrate Au(111)) (Brunetti et al., 2010; Staii et al., 2009; Acosta-García, 2005).

In vitro extracellular recording electrodes have been developed for over 30 years in order to study the electrophysiological processes occurring in both isolated and coupled excitable cells. This has led to a better understanding of the relationship between their electrical behavior and function, which in turn has allowed us to elucidate possible applications in other fields such as pharmacology. In recent years, there

https://doi.org/10.1016/j.heliyon.2018.e00550

have been important efforts aiming to culture excitable cells on substrates containing metal tracks (biochips, microelectrode arrays) in order to perform extracellular recordings of their electrical signals. Gold, in its pure or modified state was among the most used metals in these experiments (Nam et al., 2004; Heller et al., 2005; Brunetti et al., 2010; Mrksich et al., 1996; Romanova et al., 2006; Soussou et al., 2007; Coletti et al., 2009; Yoon and Mofrad, 2011).

In general, cell cultures are grown on suitable substrates to ensure proper adhesion and cell proliferation. Normally, gold tracks are added to the recording electrodes to measure the electrophysiological behavior of cells (Lin et al., 2008). A common variation of this technique consists in using gold spot electrodes instead of tracks. For this purpose, gold hemispheres have been designed to increase the contact surface between the recording electrode and the cell membrane (Hai et al., 2009). These techniques have allowed both extracellular and intracellular recordings of the electrical signals and have shown promising results (Fertig et al., 2002; Xie et al., 2012).

In summary, gold has proven to be an excellent electrical conductor for the recording of the electrical signals of cells. Moreover, evidence suggests that it does not have negative effects on cultured cells. Studies performed to discard harmful effects of gold were focused mainly on the morphology of the cells. In most cases, gold substrates were suitable for performing electrophysiological experiments at the cellular level (Nam et al., 2004; Brunetti et al., 2010; Xie et al., 2012; McAdams et al., 2006; Heller et al., 2005). For these reasons, a study of the possible effects of gold on the electrical properties of excitable cells is needed.

Voltage-clamp and current-clamp techniques have been extremely valuable for the electrophysiological characterization of excitable cells (Hille, 2001; Marty and Neher, 1995; Purves, 1981). However, these techniques are known to have several important limitations that have been the subject of intensive research for decades. For instance, when studying cells with large membrane currents (I_m) using the current-clamp technique, a voltage drop caused by I_m itself and the resistance originated by the electrolytic bath solution (in which cells are immersed during the experiments), introduce an undesirable error in the measurement of the membrane potential (V_m) (Purves, 1981; The Axon Guide, 2012). This resistance is equivalent to an additional resistor in series between the cell and ground, which often results in an additional source of error when measuring V_m, since the voltage measured in the current-clamp mode is, in fact, the sum of V_m and the voltage drop across the resistance of the electrolytic bath. This problem is accentuated when the membrane current (I_m) increases significantly because it also increases the voltage drop across the bath solution (Purves, 1981; The Axon Guide, 2012). Another important limitation is that these techniques do not allow us to obtain simultaneous high-quality recordings (i.e. with good signal to noise ratio) of the action potentials and the underlying ionic currents (Dietrich et al., 2002; Banyasz et al., 2011; Barra, 1996; Bean, 2007;

https://doi.org/10.1016/j.heliyon.2018.e00550

Berecki et al., 2005; Doerr et al., 1990; Economo et al., 2010; Nowotny et al., 2006; Molnar and Hickman, 2007; Wilders, 2006). Recently, this limitation was overcome by using carbon nanotubes as a substrate for cell culturing (Morales-Reyes et al., 2016). In this work, we propose that gold substrates can be used instead of carbon nanotubes to perform simultaneous measurements of electrical activity and the underlying membrane currents. In addition, it is important to note that given the excellent conductivity of the gold substrate, it makes possible to eliminate the resistance produced by the electrolytic bath solution in electrophysiological studies.

This work is structured as follows. First, we investigated if the gold substrates used are suitable surfaces for cell culturing. Next, we evaluated the electrical response of the cells grown on the gold substrate by analyzing the voltage-dependent Na^+ (I_{Na+}) and K^+ (I_{K+}) currents, which are mainly responsible for the generation of action potentials. Then, we use the gold substrate as an electrode by connecting it to virtual ground, which ensures a zero voltage in the immediate vicinity of the cell membrane, thus preventing the flow of ions to ground through the bath solution, which introduce an error in the measurement of V_m in electrophysiological experiments. Finally, we show how the use of this electrode allowed us to perform simultaneous recordings of the electrical activity and the underlying ionic currents, which represents an important improvement over the standard patch-clamp and other similar techniques.

2. Material and methods

2.1. Gold substrate (Au(111))

Gold substrate (Gold Arrandee TM, Au(111)) was used for culturing NG108-15 cells (Fig. 1*). The substrate area was about 1 cm^2 and 0.8 mm thick. It was cleaned by immersion in pure water (milliQ) and subjected to ultrasonic treatment for 5 minutes in absolute ethanol. Gold substrate was electrically connected to a silver wire (AGT0510 WPI USA) of 30 mm length with carbon conductive paint (Pelco 16053, Ted Pella Inc., USA) to build the electrodes.

The system was allowed to dry at room temperature for approximately 12 hrs. Electrical continuity between the silver wire and the gold substrate was verified and measured before usage. In order to achieve better mechanical support and electrical isolation, the connections and the silver wire were coated with Sylgard (SYLG184 WPI, USA). Then, it was placed on an electrical grid at a temperature of 60−80 °C for 5 minutes to accelerate the curing process. The substrate was sterilized (before being used for cell culturing) by autoclaving at 15 lbs., 140 °C for 20 minutes and then exposed to ultraviolet light for 5 minutes.

https://doi.org/10.1016/j.heliyon.2018.e00550

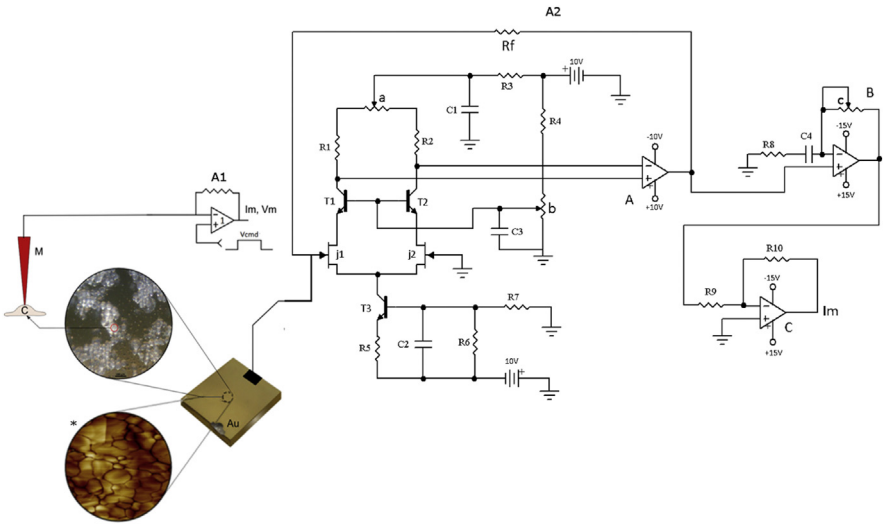

Fig. 1. Diagram of the experimental setup showing the two patch-clamp systems and the cells grown on the gold substrate. (C) Indicates the cell under study. Amplifier A1 was used to perform the standard voltage or current clamp experiments using a micropipette (M) while Amplifier A2 is used to maintain the gold substrate at virtual ground. (R) resistances, (C) capacitances, (T) 2N4401 transistor, (J) U430 FET transistor, (A, B, C) LF356 Op-Amp., (Rf) Current-voltage converter feedback resistance (100 MΩ), (I_m) output current. Potentiometers in A: (a) is used to adjust the bias current to zero, (b) is used to improve the signal to noise ratio. Potentiometer (c) in B does the frequency compensation (increase the bandwidth in the current-voltage converter). *Gold substrate with an area of 1 cm^2. Structural details of a of 200 μm^2 surface obtained by atomic force microscopy are shown (zoom). It consists of gold grains with a diameter of about 1−2 μm. Note that the grain surface is atomically flat.

2.2. Cell culture

The NG108-15 cell line was acquired from ATCC (Lot No. 58078652). NG108-15 cells were grown in monolayer cultures on plastic Petri dishes containing Dulbecco's Modified Eagle Medium (DMEM, Gibco, cat. 21063029) supplemented with 10% fetal bovine serum (FBS Gibco, cat No. 160000), 1% L-glutamine, 0.1 mM hypoxanthine, 400 nm aminopterin, 0.016 mM thymidine and 1% penicillin-streptomycin (GIBCO, cat. No. 15140) in a humidified incubator equilibrated with 5% CO_2 and 95% air at 37 °C. Cells were subcultured 15−20 times before grown in both plastic Petri dishes (control) and on the gold substrates.

2.3. Cell culture on the gold substrate

The gold substrate was placed in a plastic Petri dish (Corning 35 mm). Supplemented DMEM culture medium was added until the substrate surface was covered. The substrate was then maintained at 37 °C in an atmosphere of 5% CO_2 and 95% air for 2 hours before seeding. NG108-15 cells were placed onto the gold substrate at a density of 1×10^5 cells/ml and afterwards were incubated for 4 days. The medium was replaced every 48 hours until the beginning of the electrophysiological experiments.

https://doi.org/10.1016/j.heliyon.2018.e00550

2.4. Atomic force microscopy (AFM)

Studies of cell morphology were performed with atomic force microscopy (AFM, Nanoscope III Multimode SPM, Digital Instruments, Santa Barbara, California), in tapping mode, with AFM tips model TESP (f silicon: 325−382 kHz, k: 20−80 N/m, Veeco), at a scan rate of 0.5 Hz.

2.5. Scanning electron microscopy (SEM)

SEM Micrographs were taken with a scanning electron microscope (JEOL JSM-5900 LV). All the samples were fixed in 5% glutaraldehyde for 2 hrs and dehydrated in 20−100% ethanol. After drying using the critical point dryer, the samples were coated with gold. The SEM was operated at 15 kV accelerating voltage, with scattered electrons at a working distance of 25 mm. SEM images (500X amplification) were digitally processed to quantify the surface area of the cells cultured over both the gold substrates and petri dishes. Surface area was computed by segmenting the cells using a threshold value; then the noise was removed with an erosion procedure, followed by a closing process applied in order to fill the holes in the region of interest. Incomplete cells at the border regions of the images were manually removed.

2.6. Electrophysiology measurements

The electrical properties of the NG108-15 cells cultured in plastic Petri dishes and on the gold substrate were evaluated. An Axopatch 200A (Axon Instruments) amplifier in the whole-cell and current-clamp configurations was used to measure V_m and I_m, respectively (Fig. 1). pClamp software (Axon Instruments) was used for stimulation control and data acquisition. Signals were acquired through a Digidata 1200 converter card (Molecular Devices, CA). Signal processing was performed in Clampfit 10.2 (Molecular Devices, CA) and GraphPad Prism 5.0 (GraphPad Software Inc., San Diego, CA, USA). The sampling rate for the INa and IK was 20.4 kHz and 2.56 kHz respectively.

Pipettes (2−4 MΩ) were filled with intracellular solution containing (in mM) 10 NaCl, 140 KCl, 1 $MgCl_2$, 11 EGTA and 10 HEPES adjusted to pH 7.2 with KOH. The bath electrolytic solution contained (in mM) 151.5 NaCl, 4.5 KCl, 2 $CaCl_2$, 1 $MgCl_2$, 5 HEPES (pH adjusted to 7.4 with NaOH). All reagents were obtained from Sigma Aldrich. Solutions were filtered using 0.2 μm filters. A comparative analysis of the resting potential (Vr), input resistance (Ri), membrane capacitance (C_m) and voltage-dependent Na^+ and K^+ currents was performed in NG108-15 cells grown on plastic Petri dishes and on gold substrate. V_r was registered in current clamp mode with $I = 0$.

Membrane capacitance was obtained using the voltage step method as described elsewhere (Lollike, 1999; Gentet et al., 2000). The capacitive current through the cell

https://doi.org/10.1016/j.heliyon.2018.e00550

membrane can be expressed as $I_c = C_m(dV_m/dt)$. Integrating both sides of this equation we obtain $\int I_c dt = C_m \int dV_m = C_m(V_{m2} - V_{m1})$, wherein this case V_{m1} is the holding potential and V_{m2} is the voltage pulse applied to the cell. We used a small hyperpolarizing pulse ($V_{m2} = -10$ mV) in order to prevent the activation of the voltage-gated ionic currents and, as a result, to only obtain the transient capacitive currents (along with a linear ionic current that was completely eliminated). Once the transient capacitive current was obtained (see Fig. 2), the capacitance of the cell membrane (typically in the pF range) was determined as $C_m = \int I_c dt/(V_{m2} - V_{m1})$, where $\int I_c dt$ is the area under the curve shown in Fig. 2. Ionic currents were normalized to cell capacitance in order to obtain the corresponding current densities, which allowed us to compare the ionic currents produced by the NG108-15 cells grown on the different substrates, regardless of the size of the cells. In these experiments, the bath solution was kept grounded. Results are presented as means ± SD. Student t-test was used to examine significant differences between groups means.

The experimental arrangement described above was modified for a second series of experiments in which I_m was measured at all times regardless the patch-clamp configuration used (voltage or current-clamp). For this purpose, a second voltage-clamp system was constructed following the specifications of Hamill O. P. et al. (Hamill et al., 1981; Sigworth, 2009). Special care was always taken to ensure that the bias current and the offset voltage were set to zero (Fig. 1). Thus, I_m was measured through the second voltage-clamp system regardless the settings used in the first amplifier (voltage or current-clamp mode). As shown in Fig. 1, Amplifier A1 was used in the whole-cell mode for voltage-clamp experiments where V_{cmd} indicates the voltage pulses applied to the cell and I_m is, in this case, the output of the Amplifier A1. When Amplifier A1 was configured in the current-clamp mode, V_{cmd} in Fig. 1 indicates the

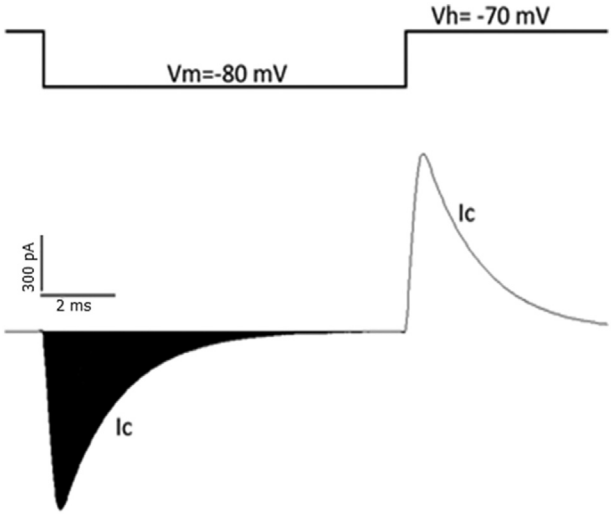

Fig. 2. The area under the curve (shaded) of the transient capacitive current (Ic) of the cell membrane of a NG108-15 cell elicited by a voltage pulse of −10 mV from a holding potential (Vh) of −70 mV.

https://doi.org/10.1016/j.heliyon.2018.e00550

current pulses applied to the cell while V_m would be the output of Amplifier A1. On the other hand, Amplifier A2 was used both to maintain the gold substrate in virtual ground and to measure I_m simultaneously. It is worth mentioning that this is possible because, in order to keep the gold substrate in virtual ground, Amplifier A2 injects a current of identical magnitude and temporal course of I_m but opposite in sign. Amplifier A1 was connected to the recording micropipette (M) while Amplifier A2 was connected to the gold substrate through a silver wire electrically isolated from the bath solution. This experimental design allowed us to measure I_m or V_m during voltage or current-clamp experiments through Amplifier A1, respectively. In addition, it was possible to simultaneously measure the course of I_m through Amplifier A2. Sampling rate for the simultaneous recording of V_m and I_m was 24.4 kHz.

3. Results

3.1. Characterization of the cell culture

To verify that gold is a suitable substrate for culturing NG108-15 cells, we evaluated the growth and the quality of the cellular material at different phases and conditions by monitoring the morphology of the cells (Fig. 3). The progress of cell growth in plastic Petri dishes and on gold substrate was monitored daily by optical microscopy (reflective mode, Fig. 3a and b, respectively). In particular, it is important to mention that cells cultured on gold substrate showed good adhesion which allowed them to proliferate to such extent that 100% confluence was reached in just 5 days. Qualitatively, no significant morphological differences between cells cultured in plastic Petri dishes and on gold substrate were observed. The size of the cells ranged between 16 to 25 μm. Well-adhered cells and dendrites growth were observed in both cultures (Fig. 3c,d,e,f). In addition, these cells showed regular and typical cell bodies which is consistent with previous reports about the morphological characteristics of the NG108-15 cells (Tojima et al., 1998, 2000a, 2000b). Areas measured from SEM images (500X) of cells cultured on Petri dishes ($1.1264 \times 10^3 \pm 0.292 \times 10^3$ μ^2, $n = 112$) and gold substrate ($1.2675 \times 10^3 \pm 0.289 \times 10^3$ μ^2, $n = 63$) did not show significant differences ($p < 0.05$). Overall, these results, obtained by different microscopy techniques, show that morphologically, cultured cells are in good conditions and well adhered to the substrate, which is particularly important to obtain adequate electrophysiological measurements.

3.2. Comparison of the passive and nonlinear electrical properties of the NG108-15 cells cultured in plastic Petri dishes and on gold substrate

Passive electrical properties of the NG108-15 cells cultured were studied in order to identify the differences between cells grown in plastic Petri dishes and on gold

https://doi.org/10.1016/j.heliyon.2018.e00550

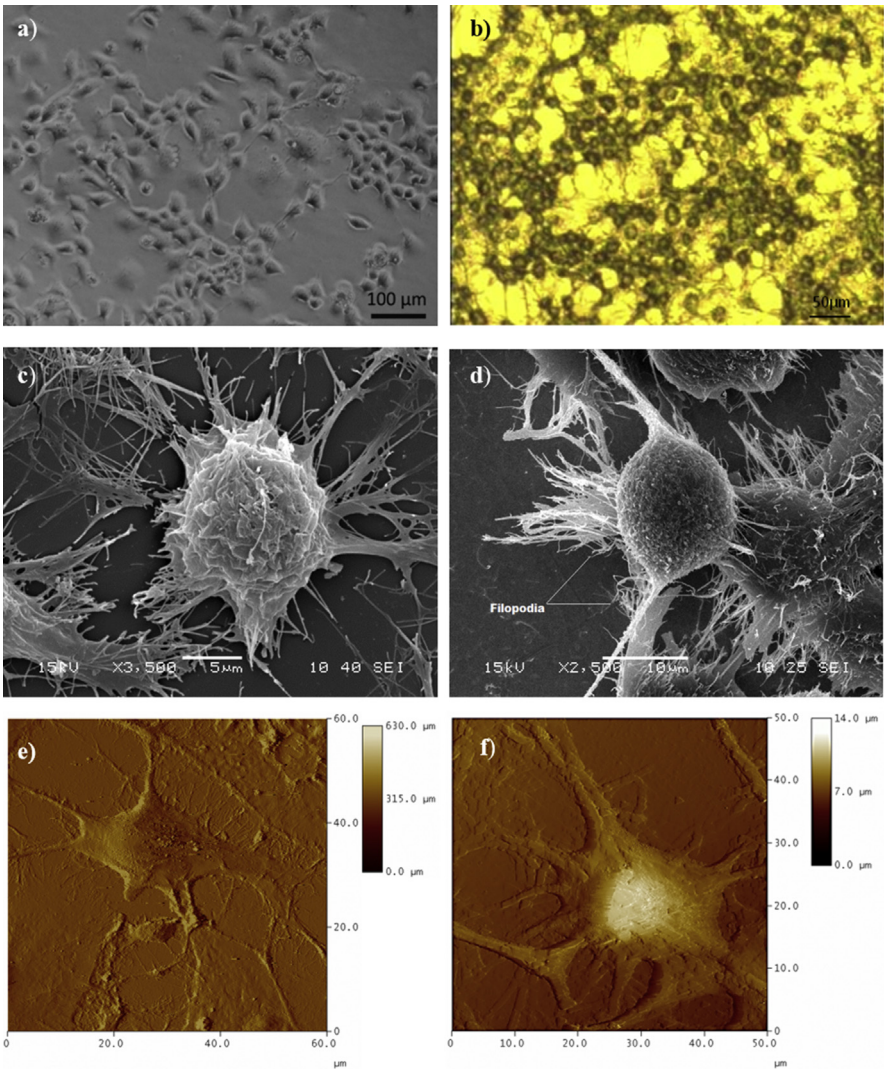

Fig. 3. Images of the NG108-15 cell culture obtained by optical microscopy at 4 days of cultivation in plastic Petri dishes (a) and on gold substrate (b). Morphological details are clearly observed in the SEM micrograph (c−d) and in the AFM image (e−f). Typical bodies, well-adhered cells and dendrites growth were observed in both cultures; the size of the cells ranged between 16 to 25 µm.

substrate. Initially, the resting potential (V_r) and input resistance (Ri) were analyzed in both substrates. V_r was measured using Amplifier 1 in current-clamp mode with the bath solution grounded (see Section 2.6). Then, the cell was polarized to −60 mV by the injection of a DC current, where current pulses of different magnitudes were applied to produce changes in the membrane potential (ΔV_m) (Fig. 4a). Voltage-current curves (ΔV_m - I_m) were constructed and fitted by linear regression (Fig. 4c). Ri was then determined by the slope of the line fitted to the ΔV_m - I_m relation. The results obtained are summarized in Table 1. The average value of the V_r measured from cells cultured on gold substrate was slightly lower in comparison to the value obtained from the cells grown in plastic dishes. In contrast, the average

https://doi.org/10.1016/j.heliyon.2018.e00550

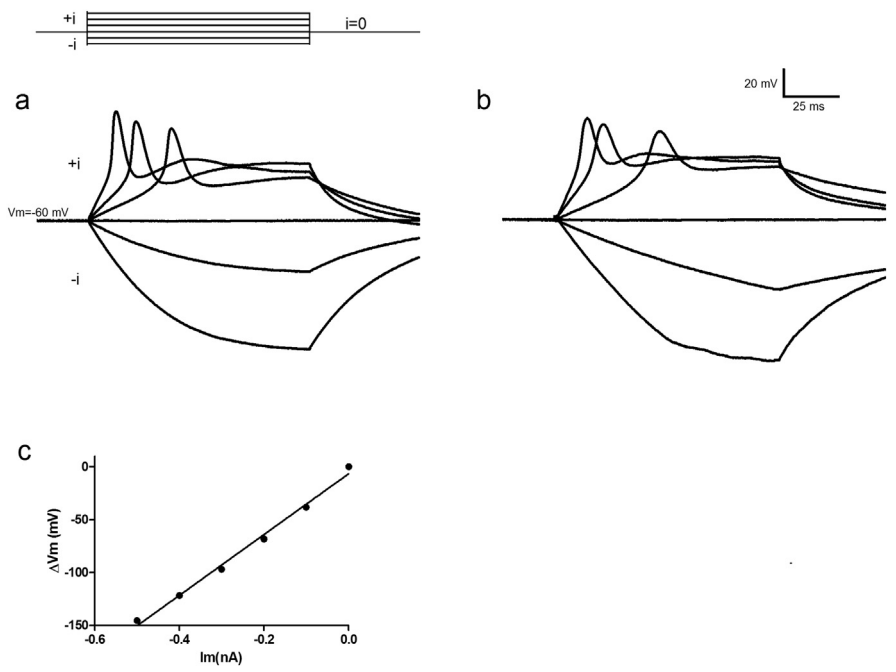

Fig. 4. Current pulses applied to the cell and the associated changes in V_m. a) Typical slow membrane potential recording obtained from cells grown on plastic Petri dishes (control). Hyperpolarizing (-i) and depolarizing (+i) current pulses were applied. The hyperpolarizing pulses produced linear changes in V_m while the depolarizing pulses produced a nonlinear response of V_m, often triggering the appearance of action potentials. b) The same protocol of current pulses was used for cells grown on gold substrate. In this case, an induced cell threshold depolarization shows a slow depolarizing-repolarizing NG108-15 voltage wave. Cells grown on both Petri dishes and gold substrate displayed slow membrane potentials when depolarizing current pulses were applied. c) The ΔV_m - I_m relation was obtained by plotting the asymptotic value of V_m against the magnitude of the corresponding hyperpolarizing pulses ($-i = I_m$), in the range where ΔV_m shows a linear behavior. The ΔV_m - I_m relation was then fitted using linear regression to obtain Ri, which is given by the slope of the fitted line.

value of the Ri of cells grown on gold substrate was larger than the one obtained in cells cultured in Petri dishes. It should be noted, however, that these differences were not statistically significant ($p > 0.05$), which allows us to conclude that the gold substrate did not affect the Ri and the V_r of the cells. On the other hand, C_m is affected in a very significant way ($p < 0.01$), being lower in the cells cultured on gold. As can be seen in Figs. 3b and 4a, depolarizing current pulses (+i) produced a nonlinear response of the V_m in cells cultured on both plastic Petri dishes (Fig. 4a) and on gold substrate (Fig. 4b). In addition, it can also be observed that the shape and magnitude of the slow depolarizing-repolarizing NG108-15 voltage wave produced were similar in both cases.

Voltage dependent Na+ and K+ currents (I_{Na+} and I_{K+}, respectively) were recorded in cells grown in both plastic Petri dishes and gold substrate using Amplifier A1 in voltage-clamp mode with the bath solution grounded (described in Section 2.6). I_{Na+} and I_{K+} were elicited by 10 and 100 ms depolarizing pulses, respectively. Due to the

https://doi.org/10.1016/j.heliyon.2018.e00550

Table 1. Passive and nonlinear electrical properties of NG108-15 cells cultured on conventional plastic Petri dishes and on gold substrate (**denotes very significant differences $p < 0.005$, the rest of the experiments show no significative differences $p > 0.05$).

	Plastic Petri dish	Gold substrate
V_r (mV)	-30.1 ± 7.21, n = 18	-26.2 ± 15.5, n = 25
Ri (MΩ)	110.6 ± 78.57, n = 14	201.4 ± 179.78, n = 20
C_m (pF)	119.9 ± 64.1, n = 10	41.6 ± 22.0, n = 10**

rapid activation of I_{Na+} and the slow activation of I_{K+}, it was possible to measure the Na^+ peak currents without the need of selective blockade of the K^+ current. Similarly, when the K^+ peak current is reached, the Na^+ current is fully inactivated already, which indicates that the K^+ peak current is not affected by the Na^+ current. This is demonstrated in Fig. 5, where both currents (recorded separately) are shown superimposed (Na^+ solid line and K^+ dashed line). The inward Na^+ current was recorded by replacing K^+ by Cs^+ in the pipette solution in order to block the K^+ current. Similarly, the K^+ current was isolated by adding Tetrodotoxin (600 nM) to the bath solution.

Results of the voltage-clamp experiments performed in cells cultured in Petri dishes are shown in Fig. 6. Negative fast-inactivating currents showing the characteristic behavior of Na^+ currents (I_{Na+}) are displayed in Fig. 6a. The peak $I_{Na+} - V_m$ relation (Fig. 6b) was used to determine the maximal Na^+ conductance for each value of

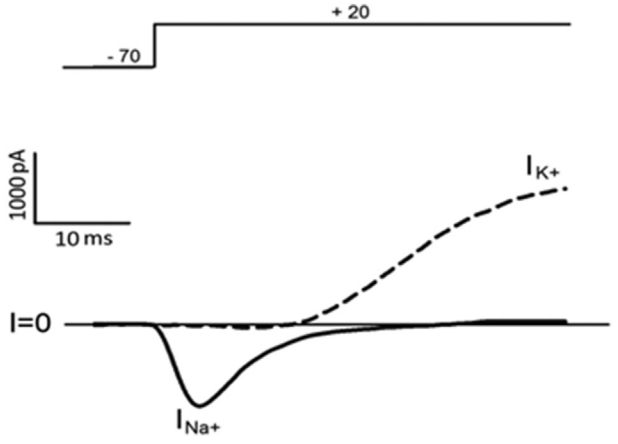

Fig. 5. Peak Na^+ and K^+ currents can be recorded without selective blockade of the Na^+ and K^+ currents respectively. Na^+ (solid line) and K^+ (dashed line) currents were elicited separately and are shown superimposed. Both currents were elicited by the voltage protocol showed above. The inward Na^+ current was recorded by replacing K^+ by Cs^+ in the pipette solution in order to block the K^+ current. Similarly, the K^+ current was isolated by adding tetrodotoxin (600 nM) to the bath solution. The numbers above indicate the depolarization of the membrane from a $V_h = -70$ mV.

https://doi.org/10.1016/j.heliyon.2018.e00550

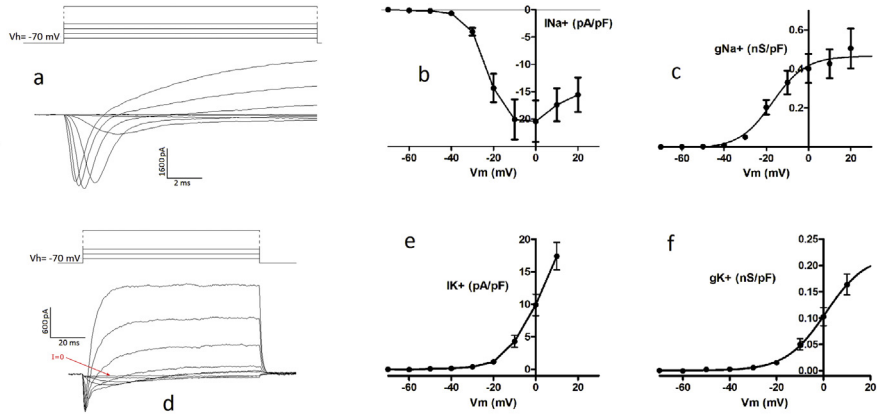

Fig. 6. Voltage clamp experiments in cells cultured on plastic Petri dishes. a) Na^+ currents elicited by 10-ms depolarizing pulses (−60 to 10 mV) from a holding potential of −70 mV. b) I_{Na+} vs. V_m curve. c) g_{Na+} vs V_m curve and the fitted Boltzmann function (smooth curve). d) K^+ currents evoked by the same protocol used in a) but using 100-ms pulses. e) I_{K+} vs. V_m curve. f) g_{K+} vs. V_m curve and the fitted Boltzmann function ($n = 10$). In b, c, e, and f data are presented as mean ± SD.

V_m ($g_{Na+} = I_{Na+}/(V_m\text{-}V_{Na+})$), where $V_{Na+} = 68$ mV is the reversal potential of Na^+ (Fig. 6c). A Boltzmann function was fitted to the resulting data points yielding a set of parameters (Table 2) that characterize the Na^+ current and the Na^+ ionic channels (Hille, 2001). The same procedure was used to analyze the K^+ current with a reversal potential $V_{K+} = -86$ mV. However, due to its slower activation process, longer depolarizing pulses (100 ms) were applied (see Section 2.6). It should be noted that, as mentioned above, measurements of I_{K+} were not contaminated by the Na^+ current since the inactivation process of I_{Na+} is much more rapid than the activation process of I_{K+} (see Fig. 5). In general, we can say that the behavior observed in Fig. 6 is similar to that previously reported in NG108-15 cells by other groups (Huang et al., 2008; Liu et al., 2012; Wu et al., 2012). The same experiments and analyses

Table 2. Parameters of the Boltzmann functions (Y = Bottom) + (Top-Bottom)/(1 + exp (V_{50}−V_m)/Slope)) fitted to the conductance-V_m relations. No significant differences between the cells grown in Petri dishes and on gold substrate were detected in the parameters obtained from the fitting procedure of the conductance-V_m relations of the Na^+ and K^+ currents (no significative differences $p > 0.05$ for all parameters).

Best-fit values	Control (Petri dishes)		Gold substrate	
	g_{Na+}-V_m (n = 10)	g_{K+}-V_m (n = 10)	g_{Na+}-V_m (n = 10)	g_{K+}-V_m (n = 10)
Bottom	0.00	0.00	0.00	0.00
Top	0.21 ± 0.14	0.26 ± 0.09	0.35 ± 0.32	0.36 ± 0.19
V_{50}	−17.60 ± 4.89	−2.40 ± 1.58	−20.75 ± 4.09	−1.80 ± 8.54
Slope	7.52 ± 2.72	7.40 ± 1.58	6.98 ± 2.30	8.90 ± 2.21

https://doi.org/10.1016/j.heliyon.2018.e00550

were done in cells cultured on the gold substrate. The Na^+ and K^+ currents produced by the same voltage-clamp protocol shown in Fig. 7, as well as the corresponding current-V_m and conductance-V_m relations are displayed in Fig. 7. It can be seen that both currents were similar to those observed for cells grown in plastic Petri dishes; that is, I_{Na+} presented both rapid activation and inactivation processes and I_{K+} showed a slow activation and a complete absence of inactivation (compare Figs. 6 and 7). Moreover, the conductance$-V_m$ relations (see Fig. 7c and f), as well as the parameters obtained from the fitting procedure (Table 2), were also similar. It is worth mentioning that to be able to compare the registered currents in cells grown on plastic Petri dishes and on gold substrate, we use the current densities obtained by normalizing the measured current to the cell capacitance (since the cell capacitance is proportional to the cell area). The parameters obtained from the fitting procedure of Boltzmann functions to the conductance-V_m relations were also compared in order to identify possible differences in the electrical response between the cells of both cultures.

So far, we found no significant differences between the cells cultured on plastic Petri dishes and on gold substrate, although C_m is in fact affected in a very significant way. In the next section, we show that it is possible to use a gold substrate to perform electrophysiological measurements in NG108-15 cells, allowing us to record action potentials (through the recording pipette) and the underlying ionic currents (recorded through the gold substrate) simultaneously. The relevance of this methodology based on the proposed experimental technique is discussed below.

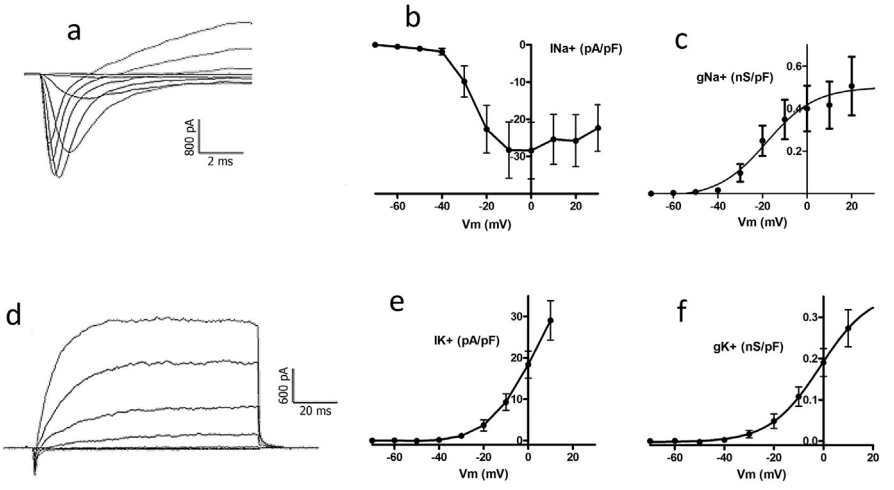

Fig. 7. Voltage-clamp experiments in cells cultured on gold substrate. a) Na^+ currents elicited by 10 ms depolarizing pulses (-60 to 10 mV) from a holding potential of -70 mV. b) I_{Na+} vs. V_m curve. c) g_{Na+} vs V_m curve and the fitted Boltzmann function (smooth curve). d) K^+ currents evoked by the same protocol used in a) but using 100 ms pulses. e) I_{K+} vs. V_m curve. f) g_{K+} vs. V_m curve and the fitted Boltzmann function ($n = 10$). In b, c, e, and f data are presented as mean $\pm$ SD.

https://doi.org/10.1016/j.heliyon.2018.e00550

3.3. Recording the membrane current through a second voltage-clamp system

All the previous current and voltage-clamp experiments were carried out using the standard electrophysiological techniques; that is, with the recording micropipette connected to Amplifier 1 and the bath solution grounded. From now on, electrophysiological measurements were performed using a modified technique consisting in the establishment setting the gold substrate as virtual ground while measuring the ion currents through the second voltage-clamp system (Amplifier A2, Fig. 1). Initially, voltage stimuli were applied through Amplifier 1 configured in the whole-cell mode. Brief (10 ms) subthreshold voltage pulses were applied (from a holding potential of −70 mV to −50 mV) in order to observe only the leakage and fast capacitive currents. This is shown in Fig. 8A, where the fast-capacitive currents evoked at the beginning and at the end of the voltage pulse can be observed. It should be noted

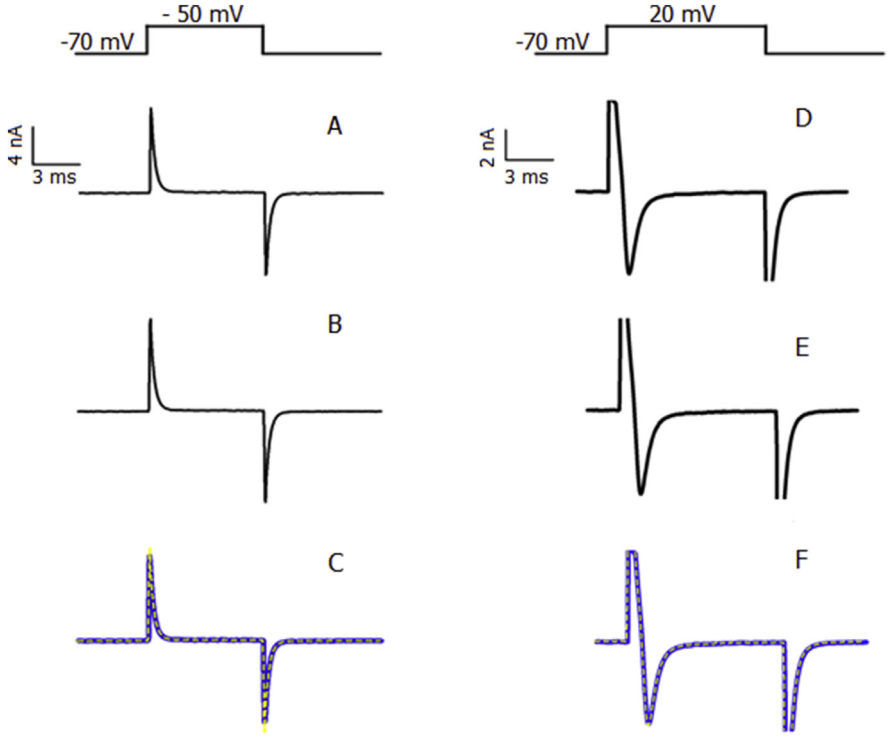

Fig. 8. A) Membrane current (I_m) evoked by a subthreshold voltage clamp pulse from a holding potential $V_h = -70$ mV to a membrane voltage of −50 mV. Only capacitive currents were observed as indicated by the transient currents observed at the start and the end of the pulse. The current was registered through the amplifier A1. B) Membrane current simultaneously recorded through the amplifier A2. C) Currents shown in (A) and (B) are displayed superimposed (solid and dotted lines, respectively). D) A greater depolarizing pulses (to 20 mV) was applied to evoke the Na^+ current (I_{Na+}). Both capacitive transient currents and the inward Na^+ current was observed. E) Current measured simultaneously through the amplifier A2. F) Currents measured through Amplifiers A1 (solid) and 2 (dashed line) are shown superimposed. Note that in D), E) and F), the capacitive currents were truncated to highlight the temporal course of I_{Na+}.

https://doi.org/10.1016/j.heliyon.2018.e00550

that the leakage current was undetectable. The current simultaneously measured through the gold substrate connected to Amplifier 2 is displayed in Fig. 8B. Notice the similarity between the current traces obtained through both amplifiers. This can be clearly appreciated in Fig. 8C were both traces are shown overlapped. Next, a depolarizing pulse of a greater magnitude (to 0 mV from a holding potential of −70 mV) were applied through Amplifier 1 to elicit the voltage-dependent Na^+ current (Fig. 8D). The current measured simultaneously through Amplifier 2 is also shown in Fig. 8E. The similarity between the two measurements can be clearly observed in Fig. 8F where both current traces are shown superimposed. It is noteworthy that Amplifier 2 faithfully follows the capacitive currents while I_{Na+} is measured with the Amplifier 1. Both are very rapid currents, and the proposed technique allowed us to obtain recordings with a good signal to noise ratio. The same results were obtained when long depolarizing pulse (100 ms) were applied to elicit and record I_{K+} (not shown).

3.4. Simultaneous measurements of the membrane potential and the membrane current

By using Amplifier A1 in the current-clamp mode and Amplifier A2 in voltage-clamp mode, while maintaining the gold substrate in virtual ground, we were able to apply current pulses and to measure the membrane potential through Amplifier A1, while at the same time, being able to measure the membrane current through Amplifier A2. Typical recordings of these simultaneous measurements of V_m and I_m are shown in Fig. 9. In the experiment shown in Fig. 9a, a negative current pulse (*) was used (blue line), resulting in the hyperpolarization of the membrane potential as expected (red line). In this particular case, the stimulating current pulse was not capable of triggering the firing of an action potential. On the other hand, when a positive current pulse (*) was applied (as indicated by the blue line in Fig. 9b), the membrane was depolarized, eventually reaching a threshold value where an action potential was produced (red line). The simultaneous measurement of the membrane current (blue line) shows the positive current pulse (*) followed by the biphasic response of the membrane currents produced by the action potential. In Fig. 9c, a temporal magnification of 9b is shown, where it is possible to discriminate between the stimulating current pulse and the temporal course of the ionic currents underlying the action potential. In Fig. 9d, a stimulating current pulse of 100 ms was imposed, which allowed us to observe $I_K{}^+$ and $I_{Na}{}^+$ added to the stimulus current pulse. In Fig. 9e, where a temporal magnification of Fig. 9d is shown, it is possible to observe the stimulating pulse and the ionic currents underlying the action potential. This biphasic behavior is produced firstly by the inward (negative) Na^+ current, followed by the outward (positive) K^+ current. As expected, the depolarization and repolarization phases of the action potential (red line) are associated to the Na^+ and K^+ currents respectively. The fast I_{Na+} that originates the depolarizing phase of the action

https://doi.org/10.1016/j.heliyon.2018.e00550

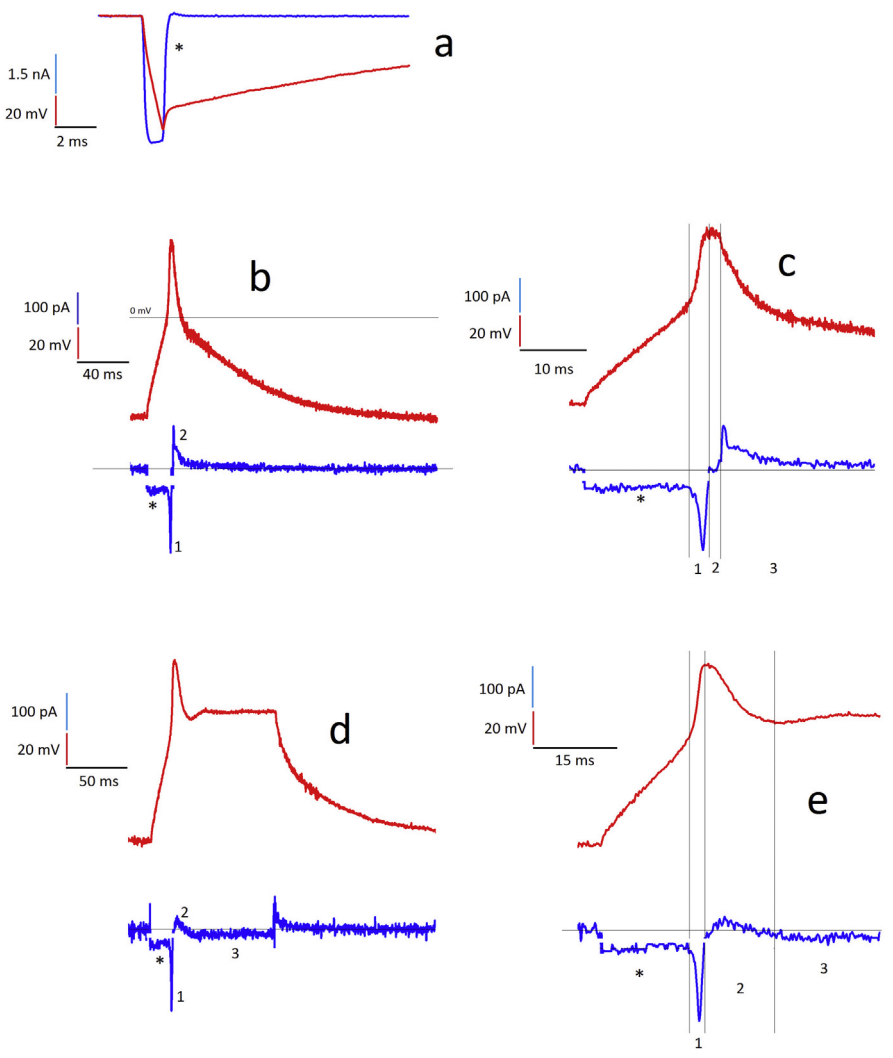

Fig. 9. Simultaneous measurement of I_m and V_m. V_m, recorded through the pipette using Amplifier A1 is shown in red. I_m (blue line) was registered through the gold substrate using Amplifier A2. The asterisk (*) indicates the current stimulus applied. a) A negative current pulse (−4.9 nA, 1 ms) produced membrane hyperpolarization, preventing the appearance of action potentials or voltage-dependent activation of the ionic currents ($V_r = -47$ mV). b) A positive current pulse triggered the firing of an action potential. The biphasic signal shown after the stimulating pulse are the currents producing the action potential ($V_r = -65$ mV). c) is a temporal magnification of b) which allowed us to discriminate between the stimulating pulse and the ionic currents underlying the action potential. d) A positive stimulating current pulse of 100 ms where I_{K+}, I_{Na+} currents are added to the stimulus current pulse. e) Temporal magnification of d) which allowed us to observe the stimulating pulse and the ionic currents underlying the action potential. Note that the stimulation current were truncated in all traces.

potential shows a typical behavior. On the other hand, I_{K+} is only activated transiently, not being maintained during the repolarization phase. These results highlight the advantages of using the methodology here proposed over the conventional techniques, which only enable us to measure the membrane potential and not the underlying membrane currents.

https://doi.org/10.1016/j.heliyon.2018.e00550

4. Discussion

Images in Fig. 3 show a qualitative characterization of NG108-15 cells grown on the plastic Petri dish and on the gold substrate, where cytoplasmic extensions and regular somas can be observed. It can be seen in the AFM images, the gold substrate does not seem to interfere with the topography nor with the shape and distribution of the cultured cells. Areas measured from SEM images (500X) of cells cultured on Petri dishes and gold substrate did not show significant differences. However, membrane capacitance measurements (C_m) indicate that the surface area of cells cultured on gold substrates is significantly lower when compared to that of cells cultured on Petri dishes. This effect could be due to the presence of a higher quantity of small cytoplasmic projections (filopodia) that would be increasing the area of the cells cultured on Petri dishes. In other words, the number of filopodia would be affected by gold but not the soma size, since the soma area showed no significant difference with respect to the cells cultured on Petri dishes. Due to the great variability in sizes of the NG108-15 cells it was necessary to report the results of the currents in terms of their density, where it is presumed that the ion channels are distributed on the cell surface that includes the filopodia (Heckman and Plummer, 2013; Schwab et al., 2012).

When analyzing the passive electrical properties of the cells (i.e. Ri and V_r), we did not find significant differences between the two substrates evaluated. Regarding the production of action potentials, the NG108-15 cells did not show a homogeneous behavior. For instance, control cells presented mostly slow depolarizing-repolarizing voltage waves while rapid action potentials were only observed occasionally. It is important to mention that, in our experience, Na^+ and K^+ ionic currents, as well as the quality and magnitude of action potentials depended heavily on the culture time. However, if cell cultures were maintained longer, dendritic like processes started to grow and the voltage clamp quality decreased. For this reason, our cell culture lasted only 4 days. During this culturing period cells grown on Petri dishes and on gold substrates exhibited different kinetics and low amplitude action potentials.

Cells grown on both surfaces also exhibited similar electrical characteristics. This was shown through a quantitative analysis of the behavior of the nonlinear voltage-dependent ion channels, which consisted in analyzing the conductance-V_m curves by fitting a Boltzmann function in order to characterize the ionic currents underlying the firing of action potentials (Hille, 1994). We did not find significant differences between the fitting parameters obtained from the K^+ and the Na^+ currents obtained from cells grown on the plastic Petri dishes and on the gold substrate. These results allow us to conclude that the gold substrate do not affect the ionic currents underlying the action potentials.

https://doi.org/10.1016/j.heliyon.2018.e00550

One of the most important problems found during an electrophysiological experiment is the voltage drop across the resistance produced by the bath solution (grounded) where cells are immersed. Although special designs of current-clamp amplifiers can solve this problem partially, it would be solved entirely if there were a good electrical conductor (as gold) grounded in the immediate vicinity of the cell membrane instead of the electrolytic bath solution. This would reduce the resistance considerably by allowing the membrane current to flow directly to ground through the electrical conductor and not through the electrolytic bath solution. In this work, we solved this problem by using the gold substrate as an electrode to ground.

The use of a gold substrate along with two voltage-clamp systems, one in the conventional manner and the other keeping the gold substrate in virtual ground has several advantages. One of the most important is that such a setup allows us to measure I_m through the second amplifier regardless if the experiment is conducted in the voltage or current-clamp mode. In addition, a key aspect of this experimental configuration is that it makes possible the simultaneous measurement of the action potentials and the underlying ionic currents without the need of a special amplifier. The latter problem had been partially solved by other approaches (Dietrich et al., 2002; Banyasz et al., 2011; Barra, 1996; Bean, 2007; Berecki et al., 2005; Doerr et al., 1990; Economo et al., 2010; Nowotny et al., 2006; Molnar and Hickman, 2007; Wilders, 2006; Hille, 1994; Levitan, 1994). Very recently, it was fully solved by using carbon nanotubes (maintained at virtual ground) as a substrate for cell culturing (Morales-Reyes et al., 2016).

Here, we showed that gold substrate is a suitable and effective alternative to the carbon nanotubes with the advantage that gold, by being an excellent electrical conductor, allows the reduction of the resistance observed in electrophysiological experiments. It should be noted, however, that in contrast to what was observed in cells grown on carbon nanotubes, patch-clamp experiments are a bit more difficult to perform on gold substrate due to its opaque surface and its relatively lower adhesivity. The former problem could be solved by using the appropriate lighting conditions, and the latter by using biomolecules such as Poly-L-lysine. It is worth mentioning that with the methodology proposed, cell adhesion requires short culturing periods (a day), and not 4 days as in this work.

These results support the idea of using gold substrates as a suitable material for both electrophysiological and morphological studies of cells, although the experimenter must be aware of the possible effects of gold on the cellular morphology. These effects can be minimized by adopting short culturing periods (from hours to a day) or by the deposition of biological molecules on its surface to promote the adhesion and wellbeing of the cells on the gold substrate.

https://doi.org/10.1016/j.heliyon.2018.e00550

5. Conclusions

By being inert, conductive and atomically flat, gold substrate poses important benefits over other conventional substrates for cell culturing, design and construction of electrophysiological instrumentation as well as for AFM and SEM studies.

In this work, we observed that NG108-15 cells grown in gold substrates exhibited a typical morphology and that they were suitable to perform further electrophysiological studies, although it should be noted, however, that depending on the culture time used, gold might affect the growth of filopodia. Besides, the electrophysiological properties of these cells, acquired through conventional patch-clamp techniques, showed no significant differences in respect to the controls, although significant differences were found in C_m. Additionally, we propose that gold substrate should be used when it is or great importance to eliminate the resistance produced by the electrolytic bath (e.g. when studying cells with large current densities).

On the other hand, by using a second amplifier to maintain the gold substrate as virtual ground, it was possible to measure V_m and I_m simultaneously with a good signal to noise ratio and, even more, without interrupting the normal development of the action potential. We think that this simultaneous recording technique can be a useful tool for electrophysiological studies like those involved in the identification of specific ionic currents underlying the firing of action potentials, which is still a subject of intensive research (see for instance Refs. Banyasz et al. (2011), Berecki et al. (2005), Doerr et al. (1990), Wilders (2006)). Moreover, the proposed methodology may allow the direct observation of the effects of pharmacological agents or modulators on action potentials and the underlying ionic currents simultaneously.

Declarations

Author contribution statement

Ma Cristina Acosta-García: Performed the experiments; Wrote the paper.

Israel Morales-Reyes: Performed the experiments.

Anabel Jiménez-Anguiano, Norma Pilar Castellanos: Analyzed and interpreted the data.

Nikola Batina: Contributed reagents, materials, analysis tools or data.

Rafael Godinez: Conceived and designed the experiments; Analyzed and interpreted the data; Wrote the paper.

https://doi.org/10.1016/j.heliyon.2018.e00550

Funding statement

This work was supported by Consejo Nacional de Ciencia y Tecnología (CONACyT) grant CB-2006-1-61242, Secretaría de Ciencia, Tecnología e Innovación (SECITI, before ICyTDF) grant (ICYTDF/274/2010-12411497). Ma. Cristina Acosta-García was supported by a scholarship from CONACYT and the support from the Posgrado en Biología Experimental (212870), División CBS, UAM-Iztapalapa.

Competing interest statement

The authors declare no conflict of interest.

Additional information

No additional information is available for this paper.

References

Acosta-García, M.C., 2005. Estudio de Células del Sistema Nervioso por Microscopia de Fuerza Atómica [MsC thesis]. ENCB, IPN, México City, México.

Banyasz, T., Horvath, B., Jiang, Z., Izu, L.T., Chen-Izu, Y., 2011. Sequential dissection of multiple ionic currents in single cardiac myocytes under action potential clamp. J. Mol. Cell. Cardiol. 50, 578−581.

Barra, P.F.A., 1996. Ionic currents during the action potential in the molluscan neurone with the self-clamp technique. Comp. Biochem. Physiol. Physiol. Part A 113 (2), 185−189.

Bean, B.P., 2007. The action potential in mammalian central neurons. Nat. Rev. Neurosci. 8, 451−465.

Berecki, G., Zegers, J.G., Verkerk, A.O., Bhuiyan, Z.A., De Jonge, B., Veldkamp, M.W., Wilders, R., van Ginneken, A.C.G., 2005. HERG channel (Dys)function revealed by dynamic action potential clamp technique. Biophys. J. 88, 566−578.

Brunetti, V., Maiorano, G., Rizzello, L., Sorce, B., Sabella, S., Cingolani, R., Pompa, P.P., 2010. Neurons sense nanoscale roughness with nanometer sensitivity. Proc. Natl. Acad. Sci. U.S.A. 107 (14), 6264−6269.

Coletti, D., Scaramuzzo, F.A., Montemiglio, L.C., Pristerá, A., Teodori, L., Adamo, S., Barteri, M., 2009. Culture of skeletal muscle cells in unprecedented proximity to a gold surface. J. Biomed. Mater. Res. Part A 91 (2), 370−377.

https://doi.org/10.1016/j.heliyon.2018.e00550

Dietrich, D., Clusmann, H., Kral, T., 2002. Improved hybrid clamp: resolution of tail currents following single action potentials. J. Neurosci. Meth. 116, 55–63.

Doerr, Th., Denger, R., Doerr, A., Trautwein, W., 1990. Ionic currents contributing to the action potential in single ventricular myocytes of the Guinea pig studied with action potential clamp. Pflüg. Arch. Eur. J. Physiol. 416, 230–237.

Economo, M.N., Fernández, F.R., White, J.A., 2010. Dynamic clamp: alteration of response properties and creation of virtual realities in neurophysiology. J. Neurosci. 30 (7), 2407–2413.

Fertig, N., Blick, R.H., Behrends, J.C., 2002. Whole Cell patch clamp recording performed on a planar glass chip. Biophys. J. 82, 3056–3062.

Gentet, L.J., Stuart, G.J., Clements, J.D., 2000. Direct measurement of specific membrane capacitance in neurons. Biophys. J. 79, 314–320.

Hai, A., Dormann, A., Shappir, J., Yitzchaik, S., Bartic, C., Borghs, G., Langedijk, J.P.M., Spira, M.E., 2009. Spine-shaped gold protrusions improve the adherence and electrical coupling of neurons with the surface of micro-electronic devices. J. R. Soc. Interface 6, 1153–1165.

Hamill, O.P., Marty, A., Neher, E., Sakmann, B., Sigworth, F.J., 1981. Improved patch-clamp techniques for high-resolution current recording from cells and cell-free membrane patches. Pflüg. Arch. Eur. J. Physiol. 391 (2), 85–100.

Heckman, C.A., Plummer III, H.K., 2013. Filopodia as sensor. Cell. Signal. 25, 2298–2311.

Heller, D.A., Garga, V., Kelleher, K.J., Lee, T.C., Mahbubani, S., Sigworth, L.A., Lee, T.R., Rea, M.A., 2005. Patterned networks of mouse hippocampal neurons on peptide-coated gold surfaces. Biomaterials 26, 883–889.

Hille, B., 1994. Modulation of ion-channel function by G-protein-coupled receptors. Trends Neurosci. 17 (12), 531–536.

Hille, B., 2001. Ion Channels of Excitable Membranes. Sunderland Massachusetts USA, third ed. Sinauer Associates, Inc. QH603. I54 H54 2001.

Huang, C.W., Huang, C.C., Lin, M.W., Tsai, J.J., Wu, S.N., 2008. The synergistic inhibitory actions of oxcarbazepine on voltage-gated sodium and potassium currents in differentiated NG108-15 neuronal cells and model neurons. Int. J. Neuropsychopharmacol. 1–14.

Levitan, I.B., 1994. Modulation of ion channels by protein phosphorylation and dephosphorylation. Annu. Rev. Physiol. 56, 193–212.

https://doi.org/10.1016/j.heliyon.2018.e00550

Lin, S.P., Chen, J.J.J., Liao, J.D., Tzeng, S.F., 2008. Characterization of surface modification on microelectrode arrays for in vitro cell culture. Biomed. Microdevices 10, 99−111.

Liu, J., Tu, H., Zhang, D., Zheng, H., Li, Y.L., 2012. Voltage-gated sodium channel expression and action potential generation in differentiated NG108-15 cells. BMC Neurosci. 13, 129.

Lollike, K., Lindau, M., 1999. Membrane capacitance techniques to monitor granule exocytosis in neutrophils. J. Immunol. Meth. 232, 111−120.

Marty, A., Neher, E., 1995. Tight-seal Whole Cell Recording, in Single-channel Recording, second ed. Springer Science, New York City, USA, pp. 31−51.

McAdams, E.T., Jossinet, J., Subramanian, R., McCauley, R.G.E., 2006. Characterization of gold electrodes in phosphate buffered saline solution by impedance and noise measurements for biological applications. In: Proceedings of the 28th IEEE SaB05.2 EMBS Annual International Conference, New York City, USA.

Molnar, P., Hickman, J.J., 2007. Patch-clamp Methods and Protocols. Humana Press Inc., New Jersey USA.

Morales, R.I., Seseña, R.A., Acosta, G.M.C., Batina, N., Godínez, F.R., 2016. Simultaneous recording of the action potential and its whole-cell associated ion current on NG108-15 cells cultured over a MWCNT electrode. Meas. Sci. Technol. 27 (8), 1−15.

Mrksich, M., Chen, C.S., Xia, Y., Dike, L.E., Ingber, D.E., Whitesides, G.M., 1996. Controlling cell attachment on contoured surfaces with self-assembled monolayers of alkanethiolates on gold. Proc. Natl. Acad. Sci. U.S.A. 93, 10775−10778.

Nam, Y., Chang, J.C., Wheeler, B.C., Brewer, G.J., 2004. Gold-coated microelectrode array with thiol linked self-assembled monolayers for engineering neuronal cultures. IEEE Trans. Biomed. Eng. 51 (1), 158−165.

Nowotny, T., Szucs, A., Pinto, R.D., Selverston, A.I., 2006. StdpC: a modern dynamic clamp. J. Neurosci. Meth. 158, 287−299.

Purves, R.D., 1981. Microelectrode Methods for Intracellular Recording and Iontophoresis. Academic Press, London.

Romanova, E.V., Oxley, S.P., Rubakhin, S.S., Bohn, P.W., Sweedler, J.V., 2006. Self-assembled monolayers of alkanethiols on gold modulate electrophysiological parameters and cellular morphology of cultured neurons. Biomaterials 27, 1665−1669.

https://doi.org/10.1016/j.heliyon.2018.e00550

Schwab, A., Fabian, A., Hanley, P.J., Stock, C., 2012. Role of ion channels and transporters in cell migration. Physiol. Rev. 92, 1865–1913.

Sigworth, F.J., 2009. Electronic design of the patch clamp. In: Sakmann, B., Neher, E. (Eds.), Single-channel Recording, second ed. Springer, New York, Dordrecht, Heidelberg, London, pp. 95–126.

Soussou, W.V., Yoon, G.J., Brinton, R.D., Berger, T.W., 2007. Neuronal network morphology and electrophysiology of hippocampal neurons cultured on surface-treated multielectrode arrays. IEEE Trans. Biomed. Eng. 54 (7), 1309–1320.

Staii, C., Viesselmann, C., Ballweg, J., Shi, L., Liu, G.Y., Williams, J.C., Dent, E.W., Coppersmith, S.N., Eriksson, M.A., 2009. Positioning and guidance of neurons on gold surfaces by directed assembly of proteins using atomic force microscopy. Biomaterials 30, 3397–3404.

The Axon™ Guide, 2012. A Guide to Electrophysiology and Biophysics Laboratory Techniques, third ed. Molecular Devices. https://www.moleculardevices.com/sites/default/files/en/asset/dd/product-brochures/axon-guide-edition-3.5-sample.pdf.

Tojima, T., Hatakeyama, D., Yamane, Y., Kawabata, K., Ushiki, T., Ogura, S., Abe, K., Ito, E., 1998. Comparative atomic force and scanning electron microscopy for fine structural images of nerve cells. Jpn. J. Appl. Phys. 37, 3855–3859.

Tojima, T., Yamane, Y., Takagi, H., Takeshita, T., Sugiyama, T., Haga, H., Kawabata, K., Ushiki, T., Abe, K., Yoshioka, T., Ito, E., 2000a. Three-dimensional characterization of interior structures of exocytotic apertures of nerve cells using atomic force microscopy. Neuroscience 101 (2), 471–481.

Tojima, T., Yamane, Y., Takahashi, M., Ito, E., 2000b. Acquisition of neuronal proteins during differentiation of NG108-15 cells. Neurosci. Res. 37, 153–161.

Wilders, R., 2006. Dynamic clamp: a powerful tool in cardiac electrophysiology. J. Physiol. 576, 349–359.

Wu, S.N., Yeh, C.C., Huang, H.C., So, E.C., Lo, Y.C., 2012. Electrophysiological characterization of sodium-activated potassium channels in NG108-15 and NSC-34 motor neuron-like cells. Acta Physiol. 206, 120–134.

Xie, C., Lin, Z., Hanson, L., Cui, Y., Cui, B., 2012. Intracellular recording of action potentials by nanopillar electroporation. Nat. Nanotechnol. 7, 185–190.

Yoon, S.H., Mofrad, M.R.K., 2011. Cell adhesion and detachment on gold surfaces modified with a thiol-functionalized RGD peptide. Biomaterials 32, 7286–7296.

https://doi.org/10.1016/j.heliyon.2018.e00550